

## A novel strategy for the protective effect of ginsenoside Rg1 against ovarian reserve decline by the PINK1 pathway

Pengdi Yang<sup>a\*</sup>, Meiling Fan<sup>b\*</sup>, Ying Chen<sup>a</sup>, Dan Yang<sup>a</sup>, Lu Zhai<sup>a</sup>, Baoyu Fu<sup>a</sup>, Lili Zhang<sup>b</sup>, Yanping Wang<sup>b</sup>, Rui Ma<sup>a</sup> and Liwei Sun<sup>a,c</sup>

<sup>a</sup>The Affiliated Hospital, Changchun University of Chinese Medicine, Changchun, China; <sup>b</sup>Obstetrics and Gynecology Center, The Affiliated Hospital, Changchun University of Chinese Medicine, Changchun, China; <sup>c</sup>Key Laboratory of Active Substances and Biological Mechanisms of Ginseng Efficacy, Ministry of Education, Changchun University of Chinese Medicine, Changchun, China

### ABSTRACT

**Context:** The decline in ovarian reserve is a major concern in female reproductive health, often associated with oxidative stress and mitochondrial dysfunction. Although ginsenoside Rg1 is known to modulate mitophagy, its effectiveness in mitigating ovarian reserve decline remains unclear.

**Objective:** To investigate the role of ginsenoside Rg1 in promoting mitophagy to preserve ovarian reserve.

**Materials and methods:** Ovarian reserve function, reproductive capacity, oxidative stress levels, and mitochondrial function were compared between ginsenoside Rg1-treated and untreated naturally aged female *Drosophila* using behavioral, histological, and molecular biological techniques. The protective effects of ginsenoside Rg1 were analyzed in a *Drosophila* model of oxidative damage induced by tert-butyl hydroperoxide. Protein expression levels in the PINK1/Parkin pathway were assessed, and molecular docking and PINK1 mutant analyses were conducted to identify potential targets.

**Results:** Ginsenoside Rg1 significantly mitigated ovarian reserve decline, enhancing offspring quantity and quality, increasing the levels of ecdysteroids, preventing ovarian atrophy, and elevating germline stem cell numbers in aged *Drosophila*. Ginsenoside Rg1 improved superoxide dismutase, catalase activity, and gene expression while reducing reactive oxygen species levels. Ginsenoside Rg1 activated the mitophagy pathway by upregulating PINK1, Parkin, and Atg8a and downregulating Ref(2)P. Knockdown of PINK1 in the ovary by RNAi attenuated the protective effects of ginsenoside Rg1. Molecular docking analysis revealed that the ginsenoside Rg1 could bind to the active site of the PINK1 kinase domain.

**Discussion and conclusions:** Ginsenoside Rg1 targets PINK1 to regulate mitophagy, preserving ovarian reserve. These findings suggest the potential of ginsenoside Rg1 as a therapeutic strategy to prevent ovarian reserve decline.

### ARTICLE HISTORY

Received 26 September

2024

Revised 18 December 2024

Accepted 8 January 2025

### KEYWORDS





Ovarian reserve decline; oxidative stress; mitophagy; PINK1/Parkin pathway; ginsenoside Rg1

### Introduction


As social and life pressures increase, more women are choosing to postpone childbirth. Although this provides greater flexibility in balancing personal and professional goals, it also increases the risk of infertility due to a decline in ovarian reserve. Studies have shown that ovarian reserve peaks at birth and progressively declines with age, with a marked decrease after 35 years (Jirge 2016; Li et al. 2019). Recent epidemiological data indicate that approximately 10% of women experience decreased ovarian reserve (DOR), and nearly 50% of these cases affect women under 40 years of age. The incidence of DOR has increased annually, with a trend towards younger populations being affected, attributed to factors such as environmental pollution, psychological stress, immune disturbances, and gynecological surgical procedures (Devine et al. 2015; Björvang et al. 2021;

Dogan et al. 2021; Luderer et al. 2022). To address the conflict between reproductive aspirations and age-related ovarian decline, many women have turned to exogenous estrogen therapy or assisted reproductive technologies. However, these interventions often carry risks, including hypertension and suboptimal ovarian responses (Levi et al. 2001). Consequently, the need for effective treatments and medications to restore ovarian function remains a pressing issue.

As women age, their ovarian antioxidant defenses decline, resulting in the excessive accumulation of reactive oxygen species (ROS) and oxidative damage, which accelerates the deterioration of ovarian reserve function (Lim and Luderer 2011; Song et al. 2016). ROS overproduction is associated with mitochondrial dysfunction, characterized by disrupted electron transport chain activity, impaired ATP synthesis, and impaired mitochondrial membrane potential (MMP), as mitochondria are the primary

**CONTACT** Rui Ma, Professor  [marujilin@163.com](mailto:marujilin@163.com)  Research Center of Traditional Chinese Medicine, the Affiliated Hospital to Changchun University of Chinese Medicine, 1478 Gongnong Street, Changchun, Jilin130021, China; Liwei Sun, Professor  [sunnyliwei@163.com](mailto:sunnyliwei@163.com)  Research Center of Traditional Chinese Medicine, the Affiliated Hospital to Changchun University of Chinese Medicine, 1478 Gongnong Street, Changchun, Jilin130021, China

\*These authors contributed equally to this work.

 Supplemental data for this article can be accessed online at <https://doi.org/10.1080/13880209.2025.2453699>.

© 2025 The Author(s). Published by Informa UK Limited, trading as Taylor & Francis Group

This is an Open Access article distributed under the terms of the Creative Commons Attribution-NonCommercial License (<http://creativecommons.org/licenses/by-nc/4.0/>), which permits unrestricted non-commercial use, distribution, and reproduction in any medium, provided the original work is properly cited. The terms on which this article has been published allow the posting of the Accepted Manuscript in a repository by the author(s) or with their consent.

sites of ROS generation (Wang et al. 2018; Zhang et al. 2019). Thus, maintaining mitochondrial function is a crucial target to improve ovarian reserve.

Mitophagy, a protective mechanism that maintains mitochondrial health and function, involves the degradation of damaged or dysfunctional mitochondria through lysosomal pathways (Kim et al. 2023; Wang, Long, et al. 2023). Emerging evidence indicates that certain natural products can regulate mitophagy in various diseases (Li, Song, et al. 2023; Luo et al. 2023). For example, resveratrol has been shown to delay oocyte aging in mice by activating mitophagy and enhancing oocyte development and ovarian reserve (Zhou et al. 2019). Additionally, Kim et al. identified the growth arrest-specific gene 6 as a regulator of mitophagy-related genes, protecting mitochondrial activity and function in mouse oocytes (Kim KH et al. 2019). These findings support the notion that mitophagy may play a role in repairing ovarian reserve function. The PINK1/Parkin pathway is the primary regulatory mechanism of mitophagy (Yu et al. 2021), with PINK1, a PTEN-induced putative kinase, acting as a critical activator of mitophagy (Venkatachalam et al. 2020; Sonn et al. 2022). This study aimed to investigate the role of PINK1-mediated mitophagy in preserving and protecting ovarian reserve function.

Ginsenoside Rg1, a tetracyclic triterpenoid saponin and the primary active component of *Panax ginseng* C. A. Meyer (Araliaceae) has shown extensive pharmacological properties, including the regulation of autophagy and antioxidant effects (Zhang et al. 2021; Zhu et al. 2022; Xie et al. 2023; Yang SJ et al. 2023). Previous studies have shown that ginsenoside Rg1 increases antioxidant enzyme levels, such as SOD and CAT, to alleviate D-galactose-induced ovarian aging in mice (Liu XH et al. 2022). Moreover, ginsenoside Rg1 has been reported to upregulate the expression of follicle-stimulating hormone receptors and downregulate senescence-related proteins, improving fertility, ovarian morphology, and hormone secretion in mice with premature ovarian failure (POF) through enhanced antioxidant capacity (He et al. 2017). However, it remains unclear whether ginsenoside Rg1 mitigates ovarian reserve decline through the mediation of mitophagy.

This study investigated the effects of ginsenoside Rg1 on the ovarian reserve in naturally aged *Drosophila* and its influence on the oxidative capacity in an oxidative damage model. Furthermore, the study explored the role of ginsenoside Rg1 in promoting mitophagy using autophagy inhibitors and examined its specific targeting of PINK1 through gene knockdown. The findings suggest that ginsenoside Rg1 may help mitigate ovarian reserve decline and extend reproductive lifespan.

## Materials and methods

### *Drosophila* source and maintenance

The *Drosophila* were purchased from the *Drosophila* resource bank of the Experimental Center of the Affiliated Hospital of the Changchun University of Chinese Medicine (Changchun, China). The PINK1 mutant *Drosophila* (Qidong, China) was provided by Qidong Fungene Biotechnology. The *Drosophila* were reared in a cornmeal-sugar-yeast agar medium containing 8% sugar (Macklin, S818046, Shanghai, China), 10.8% cornmeal (Yuanye BioTechnology Co., Ltd., S30818, Shanghai, China), 2% agar (Biofrox, 8211GR500, Marburg, Germany), 0.5% yeast extract powder (Oxoid, LP0021B, Huntingdon, UK), and 0.5% propionic acid (Merck, 8.00605, Darmstadt, DE). Eggs, larvae, pupae, and adults from the original species *Drosophila* were cultured in an incubator controlled in a temperature range of 15–18°C and a relative humidity level of 65%. The *Drosophila* was raised at a temperature

of 24–26°C with constant humidity. All *Drosophila* were kept in a 12-h light/12-h dark cycle.

Following the experimental diagram shown in Figure 1A, five experimental groups were set up, including the young group, the older group and three ginsenoside Rg1 treatment groups. In the ginsenoside Rg1 treatment groups, ginsenoside Rg1 (Yuanye BioTechnology Co., Ltd., B21057, Shanghai, China, HPLC ≥ 98%) was administered to cornmeal-sugar-yeast agar medium at final concentrations of 0.25, 0.5, and 1 mg/mL and fed for 7 days.

TBHP (Tert-butyl hydrogen peroxide solution, Sigma-Aldrich, St. Louis, 19997, MO, USA) was administered to *Drosophila* in tubes containing food supplemented with 0.3% TBHP. For the 3MA (3-Methyladenine, MedChemExpress, HY-19312, NJ, USA) treatment, tubes containing food supplemented with 50 μM 3MA were used. In the ginsenoside Rg1 treatment group, the culture medium was supplemented with ginsenoside Rg1 to 1 mg/mL. All *Drosophila* (including those in the control and treatment groups) were exposed to TBHP, 3MA, and ginsenoside Rg1 for 7 days. For experiments involving multiple compounds, fresh food containing the supplements was provided to *Drosophila* every 2–3 days.

### Reproduction assays of *Drosophila*

Each group of *Drosophila* was placed in the respective drug medium and fed for 7 days. After this period, they were transferred to a new tube containing a basal medium to mate with male *Drosophila*. After mating, 10 female *Drosophila* were transferred to a separate test tube, where they were allowed to lay eggs for 48 h. Each treatment group consisted of 40 such tubes. The number of eggs and pupae in each tube was recorded, and the pupation rate was calculated.

### Immunofluorescence staining

The ovaries were dissected in 1× PBS and fixed in 4% PFA for 30 min. The samples were washed three times with PBST (Beyotime Biotechnology, P0226, Shanghai, China) for 10 min each. To minimize non-specific antibody binding, tissues were pre-incubated in PBST supplemented with 10% goat serum for 2 h. Following this blocking step, tissues were incubated with the primary antibody overnight at 4°C. The tissues were washed three times with PBST and re-incubated in PBST with 10% goat serum (Beyotime Biotechnology, C0265, Shanghai, China) for 30 min. Subsequently, they were incubated with secondary antibodies in the dark for 2 h. The ovaries were stained with DAPI (10 μg/mL, Solarbio, C0065, Beijing, China) for 10 min. The mature eggs and the thicker egg chambers were removed using tweezers, leaving the remaining tissue containing oogonia. This tissue was placed onto a glass slide, mounted with an anti-fade mounting medium, and sealed to prevent photobleaching. The images were captured using a Nikon C2 confocal microscope.

The following antibodies were used: mouse anti-α-Spectrin (DSHB, 3A9 (323 or M10-2), Mouse, P13395, AB\_528473, 1:20, Iowa, USA) and rabbit anti-Vasa (SCBT, sc-30210, Rabbit, P09052, AB\_793874, 1:200, California, USA) (Tao et al. 2021; Weaver and Drummond-Barbosa 2021). Secondary antibodies Alexa Fluor 488-conjugated goat anti-rabbit (Thermo Fisher Scientific, A-11034, Rabbit, AB\_2576217, 1:1000, Waltham, Massachusetts, USA) and Alexa Fluor 647-conjugated goat anti-mouse (Thermo Fisher Scientific, A-21235, Mouse, AB\_2535804, 1:1000, Waltham, Massachusetts, USA) were diluted 1:1000 in PBST containing 10% goat serum. A list of Immunofluorescence antibodies is provided in Table S1.

## Ginsenoside Rg1 alleviated Ovarian Reserve Decline in aged *Drosophila*

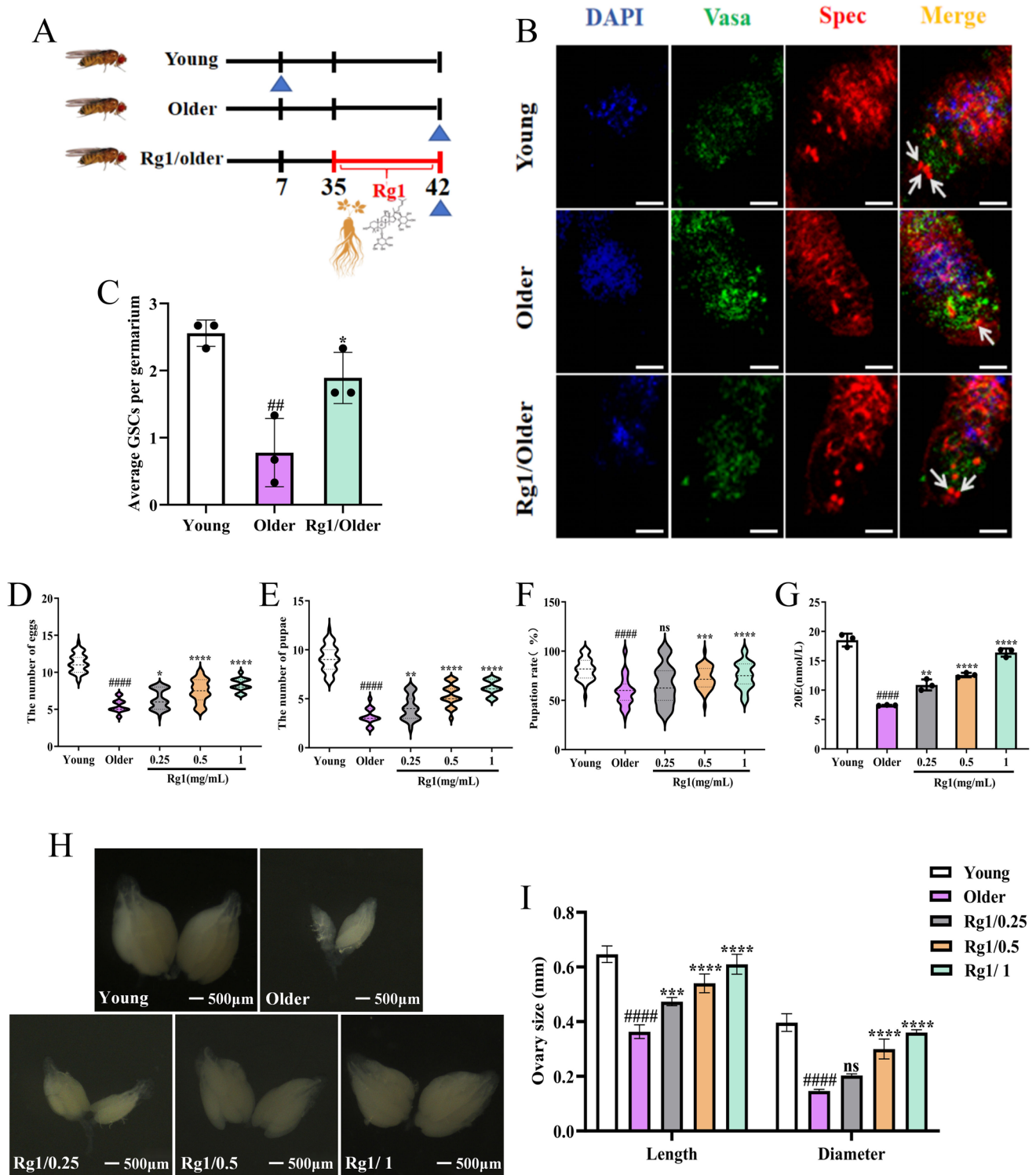


**Figure 1.** The effects of ginsenoside Rg1 on GSCs and ovarian reserve function in aged female *Drosophila*. (A) Schematic flow chart of the experiments.  $\blacktriangle$ : collecting *Drosophila*. (B) GSCs were identified by Spec staining and are illustrated by the white arrows. Scale bar: 100  $\mu$ m. (C) Quantitative analysis of GSCs. (D) The number of eggs laid by *Drosophila*. (E) The number of pupae laid by *Drosophila*. (F) The pupation rate laid by *Drosophila*. (G) 20E content in the ovary. (H) Ovary size, Scale bar = 500  $\mu$ m. (I) Length and diameter of ovary. Data are shown as the mean  $\pm$  SD.  $^{##}p < 0.001$ ,  $^{####}p < 0.0001$  compared to the young group;  $^{*}p < 0.05$ ,  $^{**}p < 0.01$ ,  $^{***}p < 0.001$ ,  $^{****}p < 0.0001$  compared to the older group.



### Determination of steroid hormone content

Following carbon dioxide anesthesia, female *Drosophila* were dissected to collect ovary samples. Using fine-tipped forceps, the ovaries were removed from each *Drosophila*. A total of 50 ovary pairs from each group were homogenized in 100 microliters of RIPA lysis buffer. The *Drosophila* tissue was homogenized using a tissue lyser (Life Real, BSH-CL2, Hangzhou, China) and centrifuged at 12000rpm for 10min. The supernatant was collected to determine the 20-hydroxyecdysone content with a Fruit fly 20-HYD ELISA KIT (Sino Best Biological Technology Co., Ltd., YX-22706F, Shanghai, China).

### Ovarian measurements

To investigate the effects of ginsenoside Rg1 on ovarian morphology, 10 female *Drosophila* in each group were selected. The *Drosophila* were euthanized by anesthetization with carbon dioxide, and their ovaries were carefully dissected at room temperature using forceps. The length and diameter of the dissected ovaries were measured in real-time using a stereomicroscope (Nikon SMZ1000 equipped with Digital Sight DS-U3, Tokyo, Japan).

### Oxidative stress status evaluation

*Drosophila* ovaries were homogenized in a 1:9 (w/v) dilution of 0.9% sodium chloride solution. The homogenate was centrifuged at 12,000g for 10min, and the supernatant was collected. The supernatant was incubated with the fluorescent probe DCFH-DA from the reactive oxygen species assay kit (Beyotime Biotechnology, S0033S, Shanghai, China) at room temperature for 60min. Fluorescence values were measured using a multi-functional enzyme reader (Tecan Infinite M200 Pro, Tecan, Männedorf, Switzerland) with an excitation wavelength of 488 nm and an emission wavelength of 525 nm. ROS levels were expressed as fluorescence intensity per mg of protein.

Ovarian tissue homogenate was used to measure superoxide dismutase (SOD, expressed as U/mg protein) and catalase (CAT, expressed as U/mg protein) activities using assay kits from Nanjing Institute of Jiancheng Bioengineering (A001-2-2 for SOD and A007-1-1 for CAT, Nanjing, China). CAT activity was assessed using the ammonium molybdate method, with absorbance recorded at 405 nm, while SOD activity was determined based on absorbance at 550 nm.

### Mitochondrial function index detection

The concentration of ATP levels in the ovaries was measured using an ATP Assay Kit (Beyotime Biotechnology, S0026, Shanghai, China). Briefly, 20 mg of ovarian tissue was lysed with 100  $\mu$ L ATP lysate and homogenized in a lyser. It was centrifuged at 12000g/min for 5 min to collect the supernatant. Next, 100  $\mu$ L of the detection working solution and 20  $\mu$ L of the sample solution were mixed into a 96-well plate. The luminescence was measured immediately with a luminometer (Thermo Fisher Scientific,

Fluoroskan Ascent™ FL, Waltham, Massachusetts, USA), and the ATP level in the sample was calculated using a standard curve.

MMP was measured based on JC-1 staining (Beyotime Biotechnology, C2006, Shanghai, China). The mitochondria in the ovarian tissue were collected using a tissue mitochondrial isolation kit and incubated with 10  $\mu$ g/mL JC-1 (Beyotime Biotechnology, C3606, Shanghai, China). Next, they were analyzed using a luminometer. The excitation and emission wavelength of the JC-1 monomer (green fluorescence) were 490 nm and 530 nm, respectively. The JC-1 polymer (red fluorescence) exhibits an excitation wavelength of 525 nm and an emission wavelength of 590 nm. The level of MMP was measured based on the relative ratio of red and green fluorescence.

Following the manufacturer's instructions from the mitochondrial complex measurement kit (Suzhou Keming Biotechnology, ml076306, ml076307, Suzhou, China), mitochondrial fractions were isolated from the samples. The activities of mitochondrial complex I and complex III were determined by measuring absorbance at 340 nm and 550 nm, respectively, using a microplate reader. The results were expressed as nmol/min/mg protein.

### Reverse transcription-quantitative PCR analysis (RT-qPCR)

Total RNA was extracted from ovarian tissue using TRIzol reagent (Thermo Fisher Scientific, 15596026CN, Waltham, Massachusetts, USA). RNA concentration was determined using Nanodrop 2000c (Thermo Fisher Scientific, Nanodrop2000C, Waltham, Massachusetts, USA). RNA was reverse transcribed to cDNA using the script cDNA synthesis kit (Bio-Rad, 12012802, CA, USA). The SYBR Premix Ex Taq Kit (Takara Biomedical Technology Co., Ltd, DRR420A, Beijing, China) and the Bio-Rad CFX96 system (Bio-Rad, 1855096, California, USA) were utilized for RT-qPCR analysis, following the manufacturer's recommended conditions and protocols. Relative mRNA expression levels were calculated using the  $\beta$ -actin-standardized  $2^{-\Delta\Delta Ct}$  formula method. A list of PCR primer sequences is provided in Table 1.

### Western blot analysis

Total protein was extracted from ovaries using a RIPA Lysis Buffer containing a PMSF solution (Beyotime Biotechnology, P0013B, ST507, Shanghai, China). The protein concentration was measured using a bicinchoninic acid (BCA) protein assay reagent (Beyotime Biotechnology, P0011, Shanghai, China). The loading control was JLA20 (DSHB, jla20, Mouse, P68139, AB\_528068, 1:2000, Iowa, USA). Subsequently, 30  $\mu$ g of total protein was mixed with 5 $\times$ loading buffer and heated at 100°C for 15 min. The samples were separated on a 12% SDS-PAGE (Bio-Rad, 1610185, California, USA) gel and transferred to a polyvinylidene difluoride membrane (PVDF, 0.22  $\mu$ m, Sigma-Aldrich, 03010040001, Missouri, USA). The membrane was first incubated with 5% skimmed milk in a blocking buffer for 1 h at room temperature to block non-specific antibody binding. Subsequently, the membrane was incubated with the primary antibody at 4°C overnight. The primary antibodies used were: PINK1 (Novus, BC100-494, Rabbit, Q9BXM7,

Table 1. Primer sequences used for RT-qPCR.

Gene	Forward (5'-3')	Reverse (5'-3')	Size (bp)	Accession number
SOD-1	GGACCGCACTTCAATCCGTATGG	GAGCGTAATCTTGGAGTCGGTGATG	106	NM_057387
SOD-2	CATCACCAGAAGCACCACCAGAC	CCATTGAAACGCAGGGCAGGAG	128	NM_001299574
CAT	GCGGATTCGACGGATCAGACTTG	GGTGGTGGTGGTGTGGTGTGG	89	NM_080483
$\beta$ -actin	TGGAGGAGGAGGAGGAGAAGTC	TTCATCTGTAGTTGGTGTGGTGTGG	112	NM_001297986



AB\_10127658, 1:1000, Colorado, USA), Parkin (Affinity, AF0235, Mouse, O60260, AB\_2833410, 1:2000, Texas, USA), Atg8a (Merck, ZRB1585, Rabbit, Q9W2S2, AB\_3665022, 1:1000, Darmstadt, DE) and Ref (2)P (Abcam, AB178440, Rabbit, P14199, AB\_2938801, 1:1000, Cambridge, UK). The PVDF membrane was incubated with the corresponding secondary antibody (ApexBio, HRP Goat Anti-Mouse/Rabbit IgG (H+L) Antibody, K1221, K1223, AB\_3665023, AB\_3665026, 1:5000, HOU, USA) at room temperature for 1 h. Finally, the protein bands were visualized and analyzed using the enhanced chemiluminescence kit (Bio-Rad, 1705070, California, USA) and the fluorchem imaging system (ProteinSimple, FluorChem E, California, USA) based on chemiluminescence.

### Molecular docking

*De novo* modeling of the active domain of PINK1 was performed using AlphaFold2, a state-of-the-art protein structure prediction tool. AlphaFold2 is known for its exceptional accuracy, predicting the 3D coordinates of all heavy atoms in a protein using the primary amino acid sequence and aligned homologous sequences as input. This advanced prediction model leverages novel neural network architectures and training strategies that integrate evolutionary relationships, physical principles, and geometric constraints intrinsic to protein structures, significantly enhancing prediction accuracy.

Molecular docking studies for small molecules were conducted using MOE Dock with the modeled active domain of PINK1. The 2D structures of the small molecules were sourced from PubChem and converted to 3D structures in MOE by energy minimization. The active domain of PINK1 served as the receptor in these simulations. Before docking, the AMBER10: the EHT force field and the Reaction Field (R-field) implicit solvation model were selected. The “induced fit” protocol was employed, allowing flexibility in the receptor binding site. This protocol permits side chains within the binding site to adjust their conformations for optimal ligand accommodation while maintaining positional constraints. The side chain tethering weight was set to 10.

Docked poses were ranked using the London dG scoring function, followed by force field refinement of the top 90 poses. These refined poses were rescored using the GBVI/WSA dG scoring function. The conformation with the lowest binding free energy was identified as the most probable binding mode. Finally, the binding mode was visualized using PyMOL.

### Statistical analysis

Data were analyzed using one-way analysis of variance (ANOVA) followed by Tukey’s multiple comparison test, conducted with GraphPad Prism 10 software. The results are presented as mean ± standard error. Statistical significance was set at  $p < 0.05$ . All experiments were performed in triplicate or more.

## Results

### Ginsenoside Rg1 alleviated ovarian reserve decline in aged *Drosophila*

Maintaining a healthy ovarian reserve depends on an adequate supply of germline stem cells (GSCs) (Ata et al. 2019; Zhou et al. 2021). In this experiment, 7-day-old young female *Drosophila* served as the control group, while 35-day-old naturally aged female *Drosophila* was used as the model group. Aged females

were treated with ginsenoside Rg1 at 0.25 mg/mL, 0.5 mg/mL, and 1 mg/mL. Our study revealed a significant decrease in GSC numbers in older female *Drosophila*, averaging only 0.78 compared to 2.56 in younger females. Treatment with ginsenoside Rg1 significantly increased the average number of GSCs in aged female *Drosophila*, increasing it to 1.89 (Figures 1B,C).

The number of eggs, pupae, and the pupation rate of the aged female *Drosophila* were significantly lower than those of the young females. However, this decrease was alleviated concentration-dependent after ginsenoside Rg1 treatment. The highest concentration (1 mg/mL) had the most pronounced effect, leading to a 49.63% increase in egg production, a 75.21% increase in pupae formation, and a 17.72% increase in pupation rate (Figures 1D–F). Furthermore, ginsenoside Rg1 effectively counteracted aging by reversing the decrease in the quantity and quality of progeny. Impaired ovarian reserve, which manifests as reduced estrogen production and ovarian atrophy, is a key indicator of aging.

The steroid hormone 20-hydroxyecdysone (20E, ecdysone) regulates the main developmental transitions in *Drosophila* (Denton et al. 2019). Ginsenoside Rg1 dose-dependently elevated ecdysone levels in aged female *Drosophila* (Figure 1G). Treatment with 1 mg/mL ginsenoside Rg1 significantly increased the length and diameter of ovaries in aged females, thereby mitigating ovarian atrophy (Figures 1H,I).

### Ginsenoside Rg1 improved aging ovarian reserve by enhancing antioxidant capacity

According to the free radical theory of aging (FRTA), excessive levels of ROS contribute significantly to the aging process (Harman 1956). ROS levels were markedly elevated in the aging ovaries, but treatment with ginsenoside Rg1 reduced these levels dose-dependently, alleviating oxidative damage (Figure 2A). The observed decline in SOD and CAT activity in aging ovaries indicates a compromised antioxidant defense system. However, ginsenoside Rg1 treatment restored the activity of both enzymes (Figures 2B,C). Additionally, the gene expression levels of the cytoplasmic antioxidant SOD1, the mitochondrial antioxidant SOD2, and CAT were significantly lower in the ovaries of older *Drosophila* compared to those of young females (Figures 2D–F). Ginsenoside Rg1 treatment significantly upregulated the expression of these antioxidant enzyme genes.

To confirm that ginsenoside Rg1 improves ovarian reserve function in aged *Drosophila* by mitigating oxidative damage, we established an oxidative damage model using TBHP (Figure 2G). Exposure to oxidative stress led to significantly impaired reproductive capacity, decreased ecdysone levels in ovarian tissue, excessive ROS production, and diminished antioxidant enzyme activity. Remarkably, ginsenoside Rg1 treatment enhanced SOD and CAT enzyme activity and gene expression, effectively scavenging excess ROS. This treatment also improved reproductive impairment and restored steroid hormone levels (Figures 2H–Q). In conclusions, ginsenoside Rg1 reduces ovarian oxidative stress in aged *Drosophila*.

### Ginsenoside Rg1 improved ovarian mitochondrial dysfunction through mitophagy

Mitochondrial dysfunction produces excessive ROS production and subsequent oxidative tissue damage (Kim et al. 2019; Yang et al. 2022). To evaluate mitochondrial function, we measured MMP and ATP levels (Li et al. 2018). In older female *Drosophila*, ovarian ATP levels and MMP were significantly reduced. Notably, treatment with ginsenoside Rg1 restored MMP and ATP

## Ginsenoside Rg1 Improved Aging Ovarian Reserve by Enhancing Antioxidant Capacity

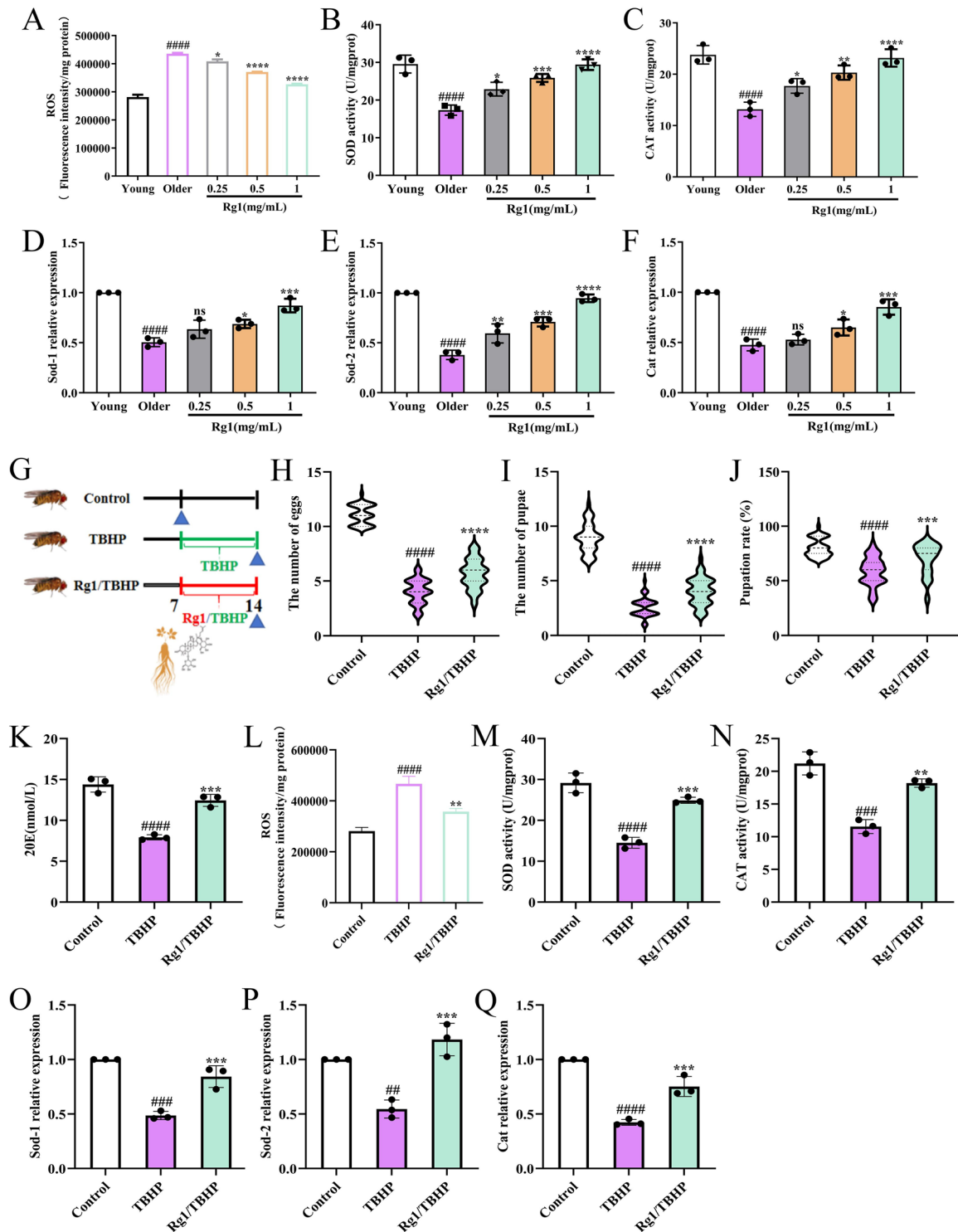


**Figure 2.** The impact of ginsenoside Rg1 on ovarian oxidative stress injury. (A) ROS levels in aging ovaries. (B and C) SOD (B), and CAT (C) enzyme activity in aging ovaries. (D–F) SOD-1 (D), SOD-2 (E), and CAT (F) of gene expression levels in aging ovaries. (G) The schematic flow chart of experiments. ▲: collecting *Drosophila*. (H) The number of eggs laid by *Drosophila*. (I) The number of pupae laid by *Drosophila*. (J) The pupation rate laid by *Drosophila*. (K) 20E content in the ovary. (L) ROS levels in oxidatively damaged ovaries. (M and N) SOD (M), and CAT (N) enzyme activities in oxidatively damaged ovaries. (O–Q) SOD-1 (O), SOD-2 (P), and CAT (Q) of gene expression levels in oxidatively damaged ovaries. Data are presented as mean ± SD. ## $p < 0.01$ , ### $p < 0.001$ , #### $p < 0.0001$  compared to the young or control group; \* $p < 0.05$ , \*\* $p < 0.01$ , \*\*\* $p < 0.001$ , \*\*\*\* $p < 0.0001$  compared to the older or TBHP-treated group.

synthesis (Figures 3A,B). ROS is predominantly generated within mitochondria through the mitochondrial respiratory chain and associated substrate dehydrogenases, with complexes I and III serving as primary production sites (An et al. 2022; Hoehne et al. 2022). The activities of mitochondrial complexes I and III were severely reduced in the aging ovaries, but ginsenoside Rg1 treatment enhanced their function (Figures 3C,D). These findings indicate that ginsenoside Rg1 effectively ameliorates mitochondrial dysfunction.

Atg8a (the *Drosophila* homolog of mammalian LC3) and Ref (2)P (the *Drosophila* equivalent of mammalian p62) are established biomarkers of autophagy (Nezis et al. 2008; Dombi et al. 2018). In the aged group, the Atg8a-II/Atg8a-I ratio and Ref (2)P levels were elevated compared to the young group. The accumulation of Ref (2)P suggested that the lysosomal capacity was insufficient to handle the increased number of damaged mitochondria. Ginsenoside Rg1 treatment significantly improved the conversion of Atg8a-I to Atg8a-II and facilitated Ref (2)P degradation (Figures 3E-I). This indicates that ginsenoside Rg1 may mitigate mitochondrial dysfunction in aging ovaries by inducing mitophagy. Furthermore, the PINK1/Parkin signaling pathway, which is essential for initiating mitophagy (Cho et al. 2021), was

significantly upregulated by ginsenoside Rg1 treatment, as evidenced by increased levels of PINK1 and Parkin proteins in aging ovaries compared to the control group.

### Ginsenoside Rg1 promoted mitophagy

To explore the effect of ginsenoside Rg1 on preserving ovarian reserve through the regulation of mitophagy, the autophagy inhibitor 3-methyladenine (3MA) was used (Figure 4A). Treatment with 3MA reduced the average number of GSCs to 1.00, indicating that inhibiting mitophagy accelerates GSC loss. However, ginsenoside Rg1 treatment restored the average number of GSCs to 2.00 (Figures 4B,C). Egg production, number of pupae, and pupation rate in *Drosophila* treated with 3MA were significantly reduced, along with a decrease in ecdysone levels. Ginsenoside Rg1 reversed these declines, restoring both reproductive capacity and ecdysone content compromised by mitophagy inhibition (Figures 4D-G). Additionally, 3MA treatment induced morphological atrophy of the ovaries, but ginsenoside Rg1 effectively restored them to normal size (Figures 4H,I). These findings suggest that the ginsenoside Rg1 promotes mitophagy and helps to maintain ovarian reserve function.

## Ginsenoside Rg1 Improved Ovarian Mitochondrial Dysfunction through Mitophagy

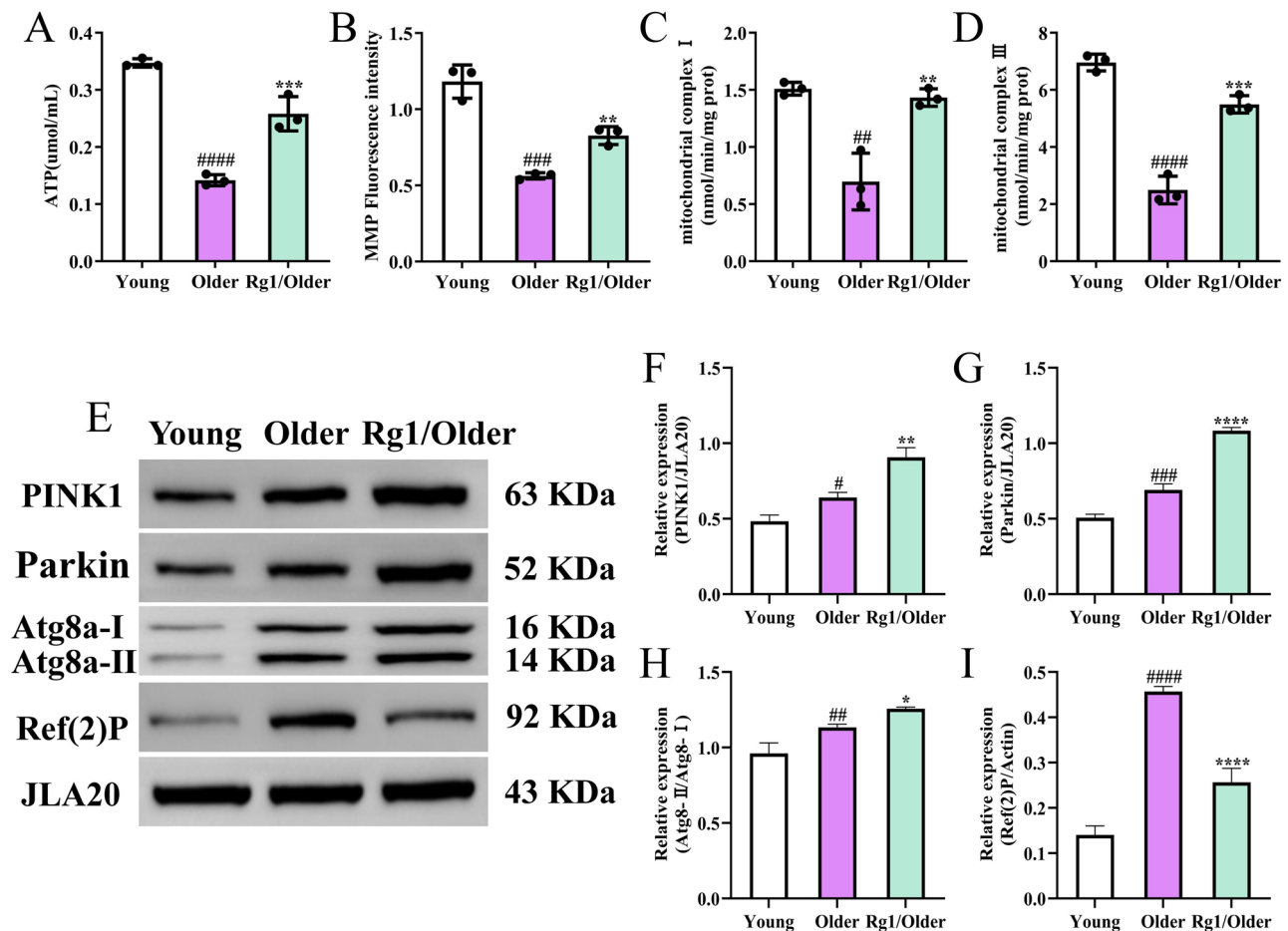


**Figure 3.** Ginsenoside Rg1 restores ovarian mitochondrial dysfunction by promoting mitophagy. (A–D) ATP (A), MMP (B), mitochondrial complex I (C), and mitochondrial complex III (D) levels in aging ovaries. (E) The effect of ginsenoside Rg1 for 7 days in aged female *Drosophila* on protein levels of PINK1, Parkin, Atg8a-II/I, and Ref (2)P in ovarian tissue as determined by Western blot. (F) The relative expression level of PINK1. (G) The relative expression level of Parkin. (H) Relative expression level of Atg8a-II/I. (I) Relative expression level of Ref (2)P. Data are shown as the mean  $\pm$  SD. # $p < 0.05$ , ## $p < 0.01$ , ### $p < 0.001$ , #### $p < 0.0001$  compared to the young group; \* $p < 0.05$ , \*\* $p < 0.01$ , \*\*\* $p < 0.001$ , \*\*\*\* $p < 0.0001$  compared to the older group.



## Ginsenoside Rg1 Promoted Mitochondrial Autophagy

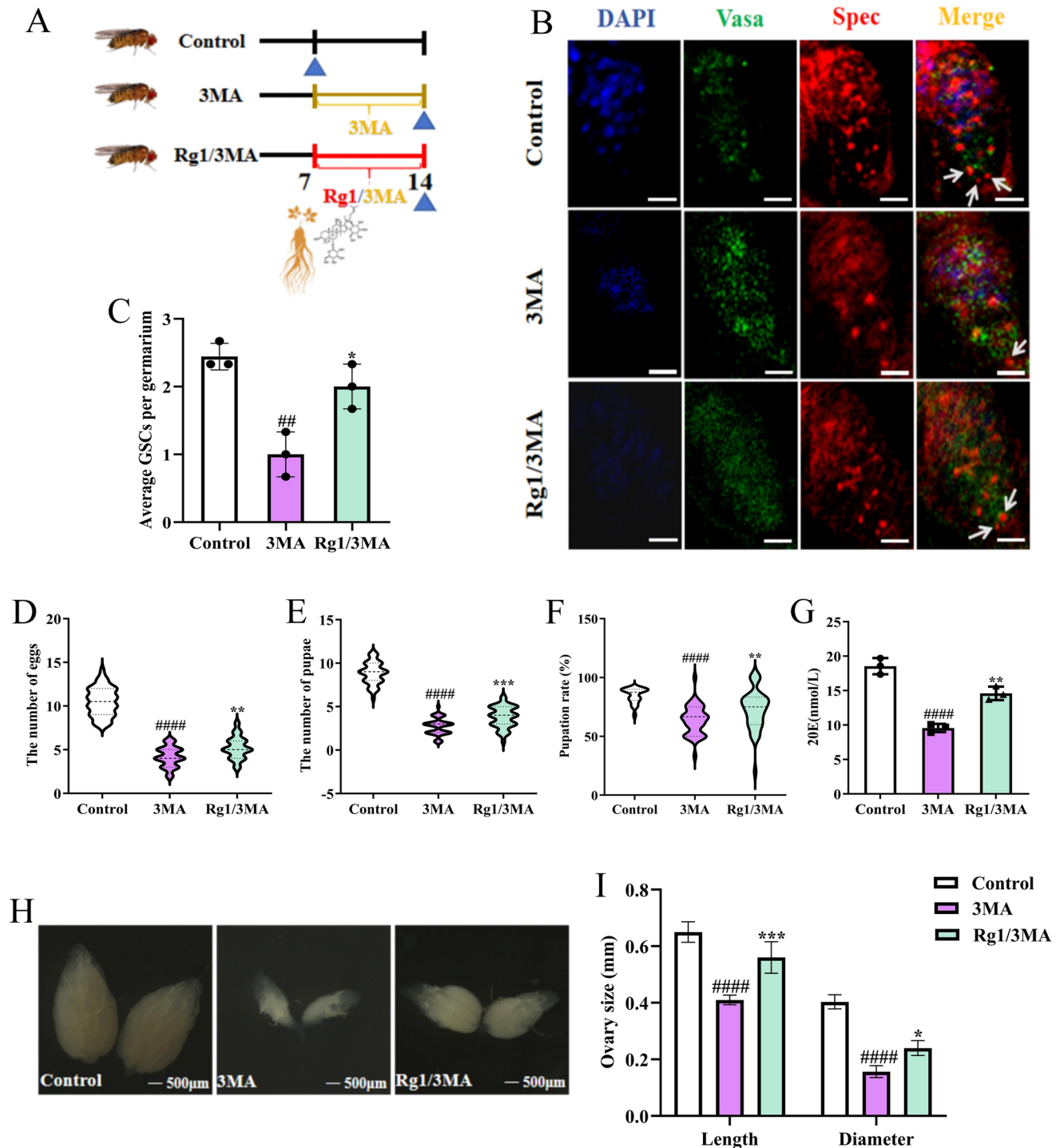


**Figure 4.** The autophagy inhibitor 3MA abolishes the effect of ginsenoside Rg1 on ovarian reserve damage. (A) Schematic illustration of the flow diagram of the experiments.  $\blacktriangle$ : collecting *Drosophila*. (B) GSCs were identified by Spec staining and are illustrated by white arrows. Scale bar: 100  $\mu$ m. (C) Quantitative analysis of GSCs. (D) The number of eggs laid by *Drosophila*. (E) The number of pupae laid by *Drosophila*. (F) The pupation rate laid by *Drosophila*. (G) 20E content in their the ovary. (H) Ovary size, Scale bar = 500  $\mu$ m. (I) Length and diameter of the ovary. Data are shown as mean  $\pm$  SD.  $##p < 0.01$ ,  $####p < 0.0001$  compared to the control group;  $*p < 0.05$ ,  $**p < 0.01$ ,  $***p < 0.001$ , compared to the 3MA group.

### Ginsenoside Rg1 dependent PINK1 activation of mitophagy improves ovarian reserve function decline

PINK1 is a “switching factor” that triggers mitophagy (Vazquez-Martin et al. 2016). To investigate its role, we used RNA interference

(RNAi) to knock down PINK1 expression in the ovaries, generating PINK1 mutant *Drosophila* (Figures 5A,B). The mean number of GSCs in control *Drosophila* was 2.56, while PINK1 mutant *Drosophila* showed a drastic reduction to only 0.67 GSCs (Figures 5C,D). PINK1 mutants exhibited significantly lower egg and pupae

## Ginsenoside Rg1 Dependent PINK1 Activation of Mitophagy Improves Ovarian Reserve Function Decline

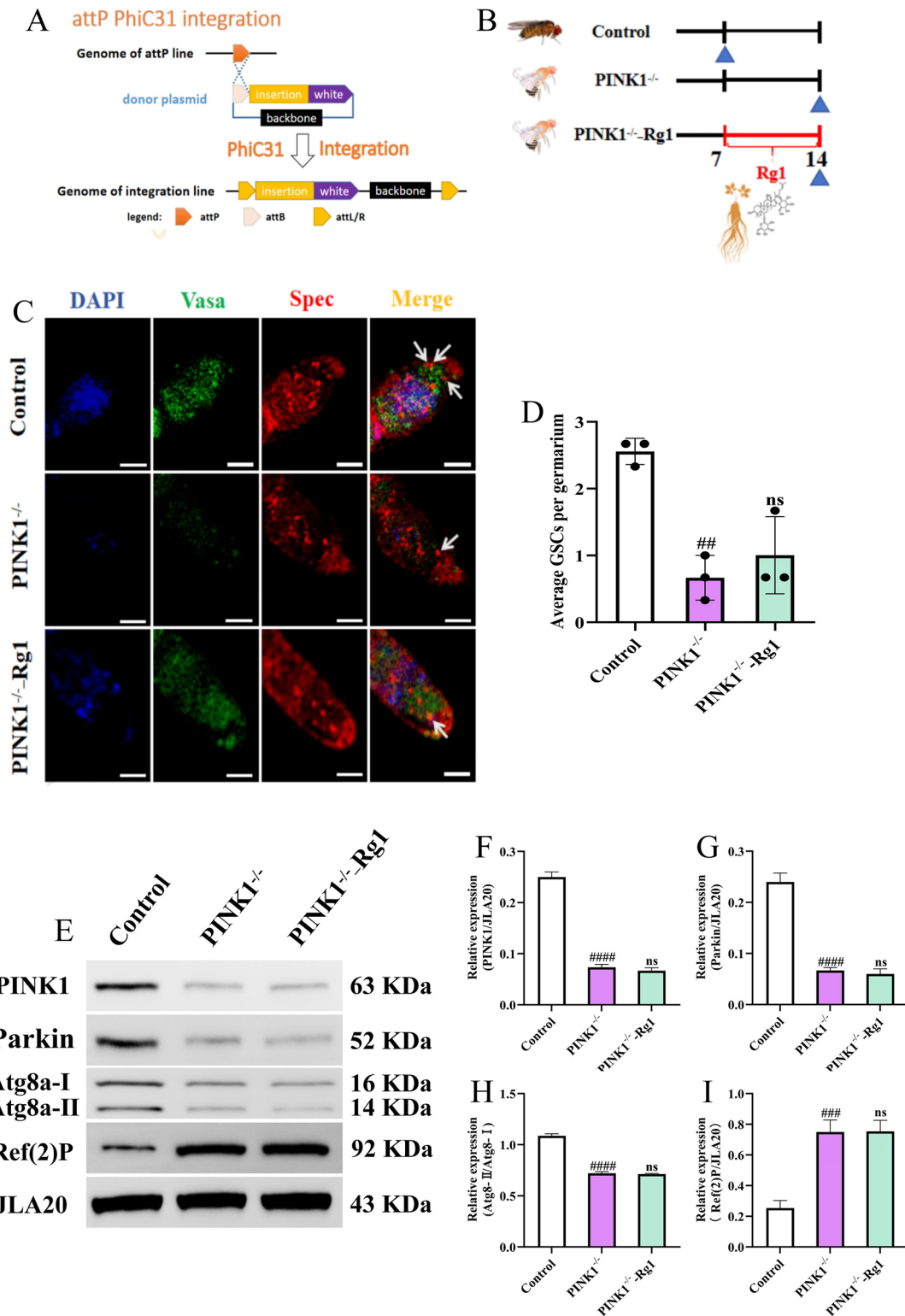


**Figure 5.** The effect of ginsenoside Rg1 on the mitophagy pathway in PINK1 mutant *Drosophila*. (A) Construction diagram of the PINK1 mutant *Drosophila*. (B) Schematic flow chart of experiments. ▲: collecting *Drosophila*. (C) GSCs were stained with Spec and are identified by the white arrows. Scale bar: 100 μm. (D) Quantitative analysis of GSCs. (E) The PINK1 mutant *Drosophila* was treated with ginsenoside Rg1 for 7 days, and the protein levels of PINK1, Parkin, Atg8a-II/I, and Ref (2)P in ovarian tissue were analyzed via Western blot. (F) Relative expression of PINK1. (G) Relative expression of Parkin. (H) Relative expression of Atg8a-II/I. (I) Relative expression of Ref (2)P. The data presented are the mean ± SD. \*\* $p < 0.01$  ### $p < 0.001$  #### $p < 0.0001$  compared to the control group; abbreviation: ns: no significance (compared to the PINK1<sup>-/-</sup> group).

## Identification of PINK1 as the Main Target of Ginsenoside Rg1

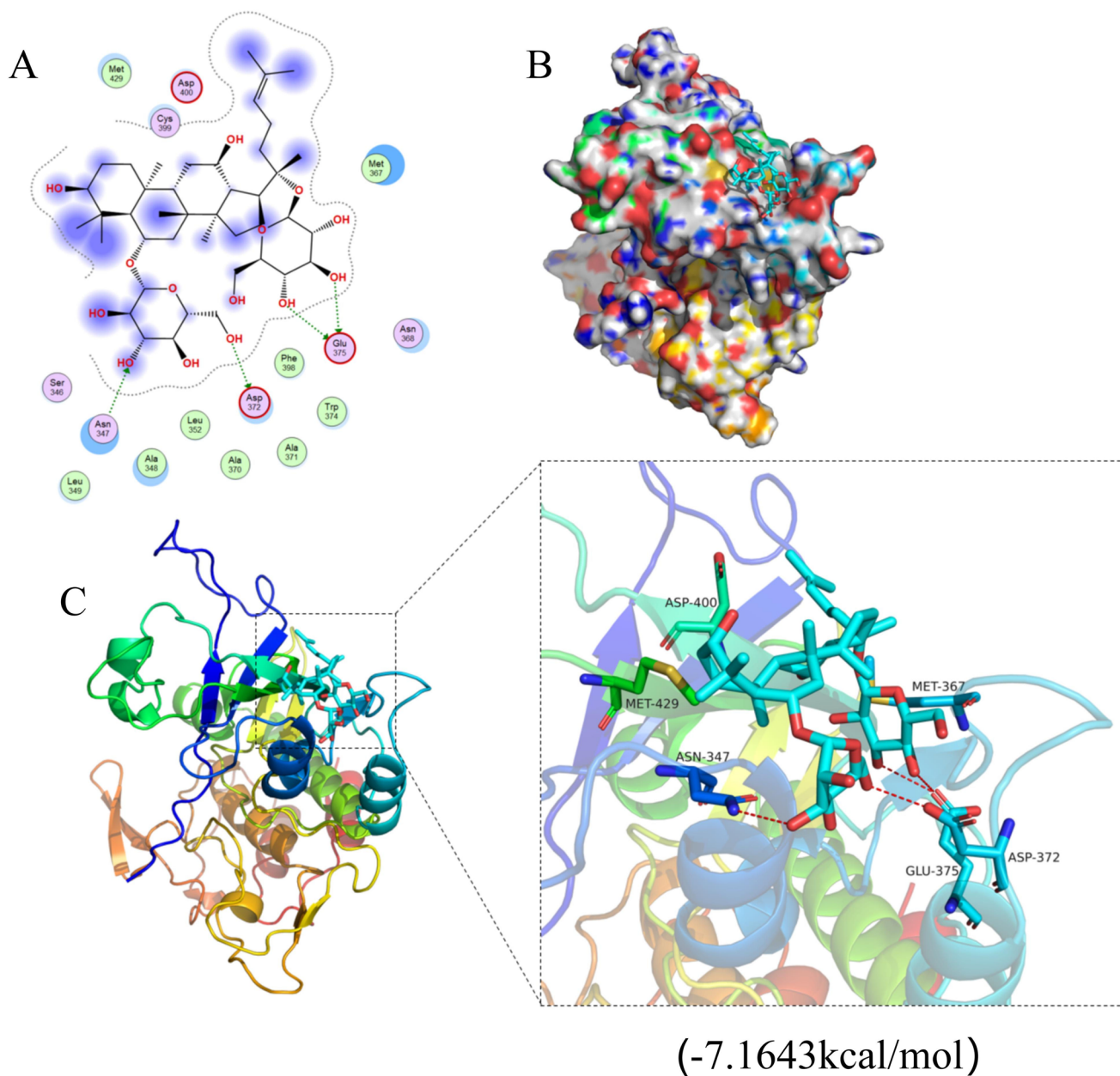


**Figure 6.** The binding model of the ginsenoside Rg1 and the active domain of PINK1. (A) The 2D binding model of ginsenoside Rg1 and the active domain of PINK1. (B) The surface binding model of ginsenoside Rg1 and the active domain of PINK1. (C) The 3D binding model of ginsenoside Rg1 and the active domain of PINK1. Ginsenoside Rg1 is indicated by the cyan color. The backbone of the receptor is depicted as a rainbow cartoon. The hydrogen bonds are illustrated by red-dashed lines.

numbers than controls, along with ovarian tissue atrophy and reduced ecdysone levels (Figures S1A–F). Ovarian mitochondrial function was severely impaired after PINK1 gene knockdown (Figures S1G–J). However, ginsenoside Rg1 treatment did not alleviate these deficiencies in the PINK1 mutant *Drosophila*. Furthermore, the expression levels of key mitophagy regulators, including PINK1, Parkin, and Atg8a, remained unaltered in the PINK1 mutants following ginsenoside Rg1 treatment, while Ref (2) P levels accumulated (Figures 5E–I). These findings indicate that the ginsenoside Rg1 activates the mitophagy pathway in a PINK1-dependent manner.

### Identification of PINK1 as the main target of ginsenoside Rg1

Molecular docking analysis is widely used to uncover interactions between compounds and proteins (Cao et al. 2022; Habib et al. 2022; Mansour et al. 2022). We conducted a molecular docking simulation to explore the potential interaction between the ginsenoside Rg1 and PINK1. The results revealed a favorable fit of ginsenoside Rg1 within the PINK1 binding pocket, indicating a potential molecular interaction. Hydrogen bonds were identified between PINK1 and ginsenoside Rg1. Specifically, the oxygen atoms in the hydroxyl groups of ginsenoside Rg1, acting as hydrogen bond donors, formed



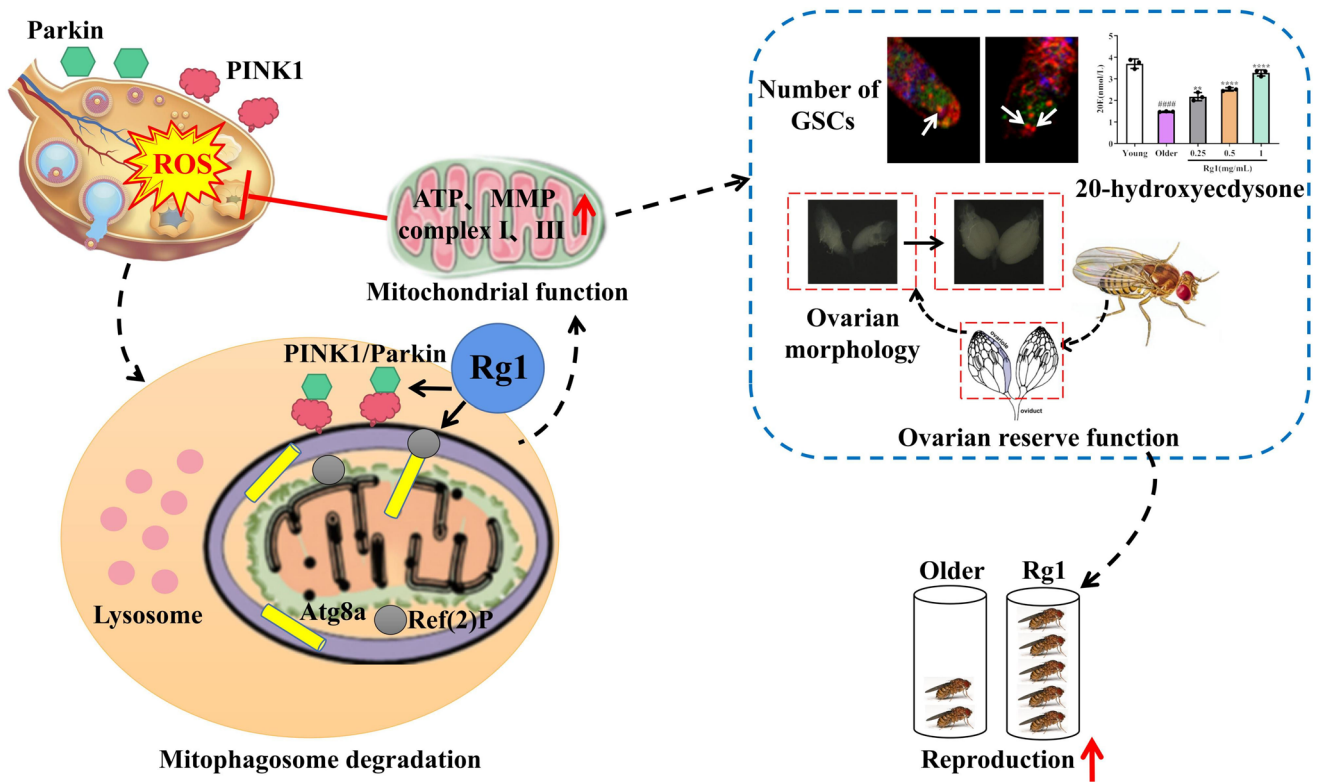


**Figure 7.** Schematic diagram showing the molecular mechanism by which mitophagy protects the ovarian reserve function in older *Drosophila*.

hydrogen bonds with the oxygen atoms in the side chains of Asp372 and Glu375 in the active domain of PINK1. Additionally, the oxygen atom in another hydroxyl group of the ginsenoside Rg1, which serves as a hydrogen bond acceptor, formed a hydrogen bond with the nitrogen atom in the side chain of Asn347 in the active domain of PINK1. Van der Waals (VDW) interactions between PINK1 and ginsenoside Rg1 also contributed to the binding. These interactions accounted for the binding energy of  $-7.1643$  kcal/mol between PINK1 and ginsenoside Rg1 (Figures 6A–C). These findings suggest that the ginsenoside Rg1 can bind to PINK1, potentially enhancing mitophagy and improving ovarian reserve.

## Discussion

The decrease in ovarian reserve is a common cause of infertility in women, particularly among those of advanced reproductive age. Increasing evidence has shown that ginsenoside Rg1, a non-hormonal natural compound, exhibits a broad spectrum of pharmacological effects, including benefits for cardiovascular disease, cancer, diabetes, and related complications (Chen et al. 2022; Cui et al. 2023; Lei et al. 2023; Liu H et al. 2024; Zhen et al. 2024). Ginsenoside Rg1 has shown promise in protecting ovarian reserve capacity under various conditions, such as diminished ovarian reserve and premature ovarian failure (Xu et al. 2021; Fu et al. 2022). In this study, ginsenoside Rg1 treatment preserved ovarian morphology, maintained hormone secretion, and restored reproductive capacity in naturally aging female *Drosophila*. It also reversed the depletion of GSCs, thereby preserving the ovarian reserve capacity in aging ovaries.

According to the free radical theory of aging, ROS-induced oxidative stress impairs the activation and development of primordial follicles, leading to the depletion of ovarian reserve (Sun et al. 2018; Asadi et al. 2022). SOD and CAT are crucial antioxidant enzymes that reflect the body's ability to neutralize free

radicals (Mei et al. 2019). Our research demonstrated a significant increase in ROS levels and a corresponding decrease in SOD and CAT activity in aging ovaries compared to those of young females, indicating redox imbalances. To further investigate the mechanisms underlying age-related ovarian reserve decline, we induced oxidative damage in *Drosophila* using TBHP, which resulted in decreased steroid hormone levels and reduced egg and pupae numbers, mimicking impaired ovarian reserve function.

Ginsenoside Rg1 treatment significantly enhanced antioxidant enzyme levels and mitigated ROS damage in naturally aged *Drosophila*. Additionally, ginsenoside Rg1 protected the reproductive capacity and oxidative stress in the TBHP-induced oxidative damage model. These findings suggest that ginsenoside Rg1 may alleviate age-related ovarian reserve decline by reducing oxidative damage.

ROS overproduction is often mediated by mitochondrial dysfunction (Takahashi et al. 2021; Jiang et al. 2022; Gao Y et al. 2023). Our study indicates that aging ovaries experience disruptions in mitochondrial complexes I and III, which are crucial regulators of ROS production. Additionally, we observed a decrease in MMP and impaired ATP synthesis, contributing to increased ROS leakage and exacerbated oxidative damage within the ovaries. Notably, ginsenoside Rg1 treatment significantly improved mitochondrial function.

A critical process for removing damaged and dysfunctional mitochondria is vital in regulating quality control and maintaining mitochondrial homeostasis (Liang et al. 2023; Mishra and Thakur 2023; Tang et al. 2023). Traditional Chinese medicines have been shown to influence mitophagy (Feng et al. 2023; Li, Jia, et al. 2023; Li, Xu, et al. 2023; Wang, Tang, et al. 2023). Autophagy is a fundamental cellular process involved in development, aging, and immunity under physiological conditions (Gao W et al. 2022; Ji et al. 2022; Shu et al. 2023). Numerous studies have shown that

natural products and traditional Chinese medicines can regulate autophagy in various diseases (Jiao et al. 2022; Mao et al. 2022; Qin et al. 2023; Shao et al. 2023; Yang N et al. 2024).

We found that aging-induced ovarian oxidative stress-activated mitophagy, as evidenced by elevated protein levels of PINK1, Parkin, and Atg8a in aging *Drosophila* ovaries. However, the Ref (2)P protein accumulation suggested that mitophagy was inhibited. Interestingly, treatment with ginsenoside Rg1 reversed this inhibition, further increasing the levels of PINK1, Parkin, and Atg8a proteins while reducing Ref (2)P levels. This suggests that ginsenoside Rg1 promotes mitophagy in aging ovaries, facilitating the degradation of impaired mitochondria and reducing oxidative damage.

Moreover, the application of the autophagy inhibitor 3MA significantly impaired ovarian reserve function. In contrast, ginsenoside Rg1 treatment activated autophagy, mitigating this impairment. These findings demonstrate that ginsenoside Rg1 protects ovarian reserve function by activating the mitophagy pathway.

PINK1 is a mitochondrial serine/threonine kinase that regulates mitophagy (Meng et al. 2022; Huang et al. 2023). Several studies have indicated that traditional Chinese medicines can enhance PINK1-associated mitophagy in various diseases (Mei et al. 2022; Zhang et al. 2023; Zhou et al. 2023). Our findings show that ginsenoside Rg1 significantly upregulated the expression of PINK1 and Parkin proteins. Molecular docking analysis using AutoDock Vina demonstrated a high binding affinity between the ginsenoside Rg1 and the active domain of PINK1, with hydrogen bonds forming between them. These results suggest that PINK1 may be an effective target for ginsenoside Rg1 to induce mitophagy.

To further investigate the relationship between PINK1 and ovarian reserve function, we used RNAi to knock down PINK1 expression in *Drosophila* ovaries. The results revealed that the PINK1 mutant *Drosophila* experienced a depletion of GSCs, ovarian atrophy, disrupted hormone secretion, and decreased reproductive capacity. Importantly, treatment with ginsenoside Rg1 did not restore the impaired ovarian reserve function in PINK1 mutant *Drosophila* nor improved the signal intensity of PINK1, Parkin, Atg8a, or Ref (2)P.

Our study demonstrates that ginsenoside Rg1 alleviates oxidative stress and supports ovarian reserve function by promoting mitophagy by targeting PINK1, ultimately prolonging reproductive lifespan (Figure 7).

## Conclusions

Oxidative stress resistance is a primary strategy for delaying aging and preventing the functional exhaustion of individual organs. Ginsenoside Rg1 protects ovarian reserve by enhancing mitophagy and reducing oxidative stress. PINK1 is identified as a critical target for improving ovarian reserve, with ginsenoside Rg1 exerting its beneficial effects through interaction with PINK1. Ginsenoside Rg1 represents a promising intervention to mitigate the decline in ovarian reserve function and extend reproductive lifespan.

## Author contributions

Conceptualization, P.Y. and L.S.; methodology, P.Y. and M.F.; validation, P.Y., M.F., Y.C., D.Y., B.F., and L.Z.; data curation, P.Y., L.Z. and R.M.; writing—original draft preparation, P.Y.; writing—review and editing, R.M. and L.S.; visualization, P.Y. and M.F.; supervision, P.Y. and Y.W.; project administration, P.Y., M.F., R.M. and L.S.; funding acquisition, R.M. and L.S.; All authors have read and agreed to the published version of the manuscript.

## Disclosure statement

The authors have declared no conflict of interest.

## Funding

This research was funded by the Natural Science Foundation of China (No. U20A20402, No. 82404993, No. 82374514) and the Science and Technology Department of Jilin Province (No. YDZJ202201ZYTS167).

## Data availability statement

The data that support the findings of this study are available from the corresponding author upon reasonable request.

## References

- An L, Zhang S, Guo P, Song L, Xie C, Guo H, Fang R, Jia Y. 2022. RIR1 represses plant immunity by interacting with mitochondrial complex I subunit in rice. *Mol Plant Pathol.* 23(1):92–103. doi: 10.1111/mpp.13145.
- Asadi E, Najafi A, Benson JD. 2022. Exogenous melatonin ameliorates the negative effect of osmotic stress in human and bovine ovarian stromal cells. *Antioxidants.* 11(6):1054. doi: 10.3390/antiox11061054.
- Ata B, Seyhan A, Seli E. 2019. Diminished ovarian reserve versus ovarian aging: overlaps and differences. *Curr Opin Obstet Gynecol.* 31(3):139–147. doi: 10.1097/GCO.0000000000000536.
- Björvang RD, Hassan J, Stefopoulou M, Gemzell-Danielsson K, Pedrelli M, Kiviranta H, Rantakokko P, Ruokojärvi P, Lindh CH, Acharya G, et al. 2021. Persistent organic pollutants and the size of ovarian reserve in reproductive-aged women. *Environ Int.* 155:106589. doi: 10.1016/j.envint.2021.106589.
- Cao G, Miao H, Wang YN, Chen DQ, Wu XQ, Chen L, Guo Y, Zou L, Vaziri ND, Li P, et al. 2022. Intrarenal 1-methoxypyrene, an aryl hydrocarbon receptor agonist, mediates progressive tubulointerstitial fibrosis in mice. *Acta Pharmacol Sin.* 43(11):2929–2945. doi: 10.1038/s41401-022-00914-6.
- Chen W, Jin X, Wang T, Bai R, Shi J, Jiang Y, Tan S, Wu R, Zeng S, Zheng H, et al. 2022. Ginsenoside Rg1 interferes with the progression of diabetic osteoporosis by promoting type H angiogenesis modulating vasculogenic and osteogenic coupling. *Front Pharmacol.* 13:1010937. doi: 10.3389/fphar.2022.1010937.
- Cho YH, Kim GH, Park JJ. 2021. Mitochondrial aconitase 1 regulates age-related memory impairment via autophagy/mitophagy-mediated neural plasticity in middle-aged flies. *Aging Cell.* 20(12):e13520. doi: 10.1111/accel.13520.
- Cui L, Liu X, Yan R, Chen Q, Wang L, Nawaz S, Qin D, Wang D. 2023. Amino acid modified OCMC-g-Suc-beta-CD nanohydrogels carrying lapatinib and ginsenoside Rg1 exhibit high anticancer activity in a zebrafish model. *Front Pharmacol.* 14:1149191. doi: 10.3389/fphar.2023.1149191.
- Denton D, Xu T, Dayan S, Nicolson S, Kumar S. 2019. Dpp regulates autophagy-dependent midgut removal and signals to block ecdysone production. *Cell Death Differ.* 26(4):763–778. doi: 10.1038/s41418-018-0154-z.
- Devine K, Mumford SL, Wu M, DeCherney AH, Hill MJ, Propst A. 2015. Diminished ovarian reserve in the United States assisted reproductive technology population: diagnostic trends among 181,536 cycles from the society for assisted reproductive technology clinic outcomes reporting system. *Fertil Steril.* 104(3):612–619.e3. doi: 10.1016/j.fertnstert.2015.05.017.
- Dogan S, Cicek OSY, Demir M, Yalcinkaya L, Sertel E. 2021. The effect of growth hormone adjuvant therapy on assisted reproductive technologies outcomes in patients with diminished ovarian reserve or poor ovarian response. *J Gynecol Obstet Hum Reprod.* 50(2):101982. doi: 10.1016/j.jog-oh.2020.101982.
- Dombi E, Mortiboys H, Poulton J. 2018. Modulating mitophagy in mitochondrial disease. *Curr Med Chem.* 25(40):5597–5612. doi: 10.2174/0929867324666170616101741.
- Feng WD, Wang Y, Luo T, Jia X, Cheng CQ, Wang HJ, Zhang MQ, Li QQ, Wang XJ, Li YY, et al. 2023. Scoparone suppresses mitophagy-mediated

- NLRP3 inflammasome activation in inflammatory diseases. *Acta Pharmacol Sin.* 44(6):1238–1251. doi: [10.1038/s41401-022-01028-9](https://doi.org/10.1038/s41401-022-01028-9).
- Fu B, Ma R, Liu F, Chen X, Teng X, Yang P, Liu J, Zhao D, Sun L. 2022. Ginsenosides improve reproductive capability of aged female *Drosophila* through mechanism dependent on ecdysteroid receptor (ECR) and steroid signaling pathway. *Front Endocrinol.* 13:964069. doi: [10.3389/fendo.2022.964069](https://doi.org/10.3389/fendo.2022.964069).
- Gao W, Wang X, Zhou Y, Wang X, Yu Y. 2022. Autophagy, ferroptosis, pyroptosis, and necroptosis in tumor immunotherapy. *Signal Transduct Target Ther.* 7(1):196. doi: [10.1038/s41392-022-01046-3](https://doi.org/10.1038/s41392-022-01046-3).
- Gao Y, Zou Y, Wu G, Zheng L. 2023. Oxidative stress and mitochondrial dysfunction of granulosa cells in polycystic ovarian syndrome. *Front Med.* 10:1193749. doi: [10.3389/fmed.2023.1193749](https://doi.org/10.3389/fmed.2023.1193749).
- Habib MR, Hamed AA, Ali REM, Zayed KM, Gad El-Karim RM, Sabour R, Abu El-Einin HM, Ghareeb MA. 2022. Thais savignyi tissue extract: bioactivity, chemical composition, and molecular docking. *Pharm Biol.* 60(1):1899–1914. doi: [10.1080/13880209.2022.2123940](https://doi.org/10.1080/13880209.2022.2123940).
- Harman D. 1956. Aging: a theory based on free radical and radiation chemistry. *J Gerontol.* 11(3):298–300. doi: [10.1093/geronj/11.3.298](https://doi.org/10.1093/geronj/11.3.298).
- He L, Ling L, Wei T, Wang Y, Xiong Z. 2017. Ginsenoside Rg1 improves fertility and reduces ovarian pathological damages in premature ovarian failure model of mice. *Exp Biol Med.* 242(7):683–691. doi: [10.1177/1535370217693323](https://doi.org/10.1177/1535370217693323).
- Hoehne MN, Jacobs L, Lapacz KJ, Calabrese G, Murschall LM, Marker T, Kaul H, Trifunovic A, Morgan B, Fricker M, et al. 2022. Spatial and temporal control of mitochondrial H(2) O(2) release in intact human cells. *Embo J.* 41(7):e109169.
- Huang JR, Zhang MH, Chen YJ, Sun YL, Gao ZM, Li ZJ, Zhang GP, Qin Y, Dai XY, Yu XY, et al. 2023. Urolithin A ameliorates obesity-induced metabolic cardiomyopathy in mice via mitophagy activation. *Acta Pharmacol Sin.* 44(2):321–331. doi: [10.1038/s41401-022-00919-1](https://doi.org/10.1038/s41401-022-00919-1).
- Ji XY, Zheng D, Ni R, Wang JX, Shao JQ, Vue Z, Hinton A, Jr., Song LS, Fan GC, Chakrabarti S, et al. 2022. Sustained over-expression of calpain-2 induces age-dependent dilated cardiomyopathy in mice through aberrant autophagy. *Acta Pharmacol Sin.* 43(11):2873–2884. doi: [10.1038/s41401-022-00965-9](https://doi.org/10.1038/s41401-022-00965-9).
- Jiang XS, Cai MY, Li XJ, Zhong Q, Li ML, Xia YF, Shen Q, Du XG, Gan H. 2022. Activation of the Nrf2/ARE signaling pathway protects against palmitic acid-induced renal tubular epithelial cell injury by ameliorating mitochondrial reactive oxygen species-mediated mitochondrial dysfunction. *Front Med.* 9:939149. doi: [10.3389/fmed.2022.939149](https://doi.org/10.3389/fmed.2022.939149).
- Jiao Y, Xin M, Xu J, Xiang X, Li X, Jiang J, Jia X. 2022. Polyphyllin II induced apoptosis of NSCLC cells by inhibiting autophagy through the mTOR pathway. *Pharm Biol.* 60(1):1781–1789. doi: [10.1080/13880209.2022.2120021](https://doi.org/10.1080/13880209.2022.2120021).
- Jirge PR. 2016. Poor ovarian reserve. *J Hum Reprod Sci.* 9(2):63–69. doi: [10.4103/0974-1208.183514](https://doi.org/10.4103/0974-1208.183514).
- Kim HY, Yoon HS, Heo AJ, Jung EJ, Ji CH, Mun SR, Lee MJ, Kwon YT, Park JW. 2023. Mitophagy and endoplasmic reticulum-phagy accelerated by a p62 ZZ ligand alleviates paracetamol-induced hepatotoxicity. *Br J Pharmacol.* 180(9):1247–1266. doi: [10.1111/bph.16004](https://doi.org/10.1111/bph.16004).
- Kim KH, Kim EY, Ko JJ, Lee KA. 2019. Gas6 is a reciprocal regulator of mitophagy during mammalian oocyte maturation. *Sci Rep.* 9(1):10343. doi: [10.1038/s41598-019-46459-3](https://doi.org/10.1038/s41598-019-46459-3).
- Kim YR, Baek JI, Kim SH, Kim MA, Lee B, Ryu N, Kim KH, Choi DG, Kim HM, Murphy MP, et al. 2019. Therapeutic potential of the mitochondria-targeted antioxidant MitoQ in mitochondrial-ROS induced sensorineural hearing loss caused by *Ihh2* deficiency. *Redox Biol.* 20:544–555. doi: [10.1016/j.redox.2018.11.013](https://doi.org/10.1016/j.redox.2018.11.013).
- Lei C, Chen J, Huang Z, Men Y, Qian Y, Yu M, Xu X, Li L, Zhao X, Jiang Y, et al. 2023. Ginsenoside Rg1 can reverse fatigue behavior in CFS rats by regulating EGFR and affecting Taurine and Mannose 6-phosphate metabolism. *Front Pharmacol.* 14:1163638. doi: [10.3389/fphar.2023.1163638](https://doi.org/10.3389/fphar.2023.1163638).
- Levi AJ, Raynault MF, Bergh PA, Drews MR, Miller BT, Scott RT Jr. 2001. Reproductive outcome in patients with diminished ovarian reserve. *Fertil Steril.* 76(4):666–669. doi: [10.1016/s0015-0282\(01\)02017-9](https://doi.org/10.1016/s0015-0282(01)02017-9).
- Li G, Xu Y, Li Y, Chang D, Zhang P, Ma Z, Chen D, You Y, Huang X, Cai J. 2023. Qiangjing tablets ameliorate asthenozoospermia via mitochondrial ubiquitination and mitophagy mediated by LKB1/AMPK/ULK1 signaling. *Pharm Biol.* 61(1):271–280. doi: [10.1080/13880209.2023.2168021](https://doi.org/10.1080/13880209.2023.2168021).
- Li J, Liu X, Hu L, Zhang F, Wang F, Kong H, Dai S, Guo Y. 2019. A slower age-related decline in treatment outcomes after the first ovarian stimulation for in women with polycystic ovary syndrome. *Front Endocrinol (Lausanne).* 10:834. doi: [10.3389/fendo.2019.00834](https://doi.org/10.3389/fendo.2019.00834).
- Li L, Jia Q, Wang X, Wang Y, Wu C, Cong J, Ling J. 2023. Chaihu Shugan San promotes gastric motility in rats with functional dyspepsia by regulating Drp-1-mediated ICC mitophagy. *Pharm Biol.* 61(1):249–258. doi: [10.1080/13880209.2023.2166966](https://doi.org/10.1080/13880209.2023.2166966).
- Li L, Song JJ, Zhang MX, Zhang HW, Zhu HY, Guo W, Pan CL, Liu X, Xu L, Zhang ZY. 2023. Oridonin ameliorates caspase-9-mediated brain neuronal apoptosis in mouse with ischemic stroke by inhibiting RIPK3-mediated mitophagy. *Acta Pharmacol Sin.* 44(4):726–740. doi: [10.1038/s41401-022-00995-3](https://doi.org/10.1038/s41401-022-00995-3).
- Li R, Xin T, Li D, Wang C, Zhu H, Zhou H. 2018. Therapeutic effect of Sirtuin 3 on ameliorating nonalcoholic fatty liver disease: the role of the ERK-CREB pathway and Bnip3-mediated mitophagy. *Redox Biol.* 18:229–243. doi: [10.1016/j.redox.2018.07.011](https://doi.org/10.1016/j.redox.2018.07.011).
- Liang S, Bao C, Yang Z, Liu S, Sun Y, Cao W, Wang T, Schwantes-An TH, Choy JS, Naidu S, et al. 2023. SARS-CoV-2 spike protein induces IL-18-mediated cardiopulmonary inflammation via reduced mitophagy. *Signal Transduct Target Ther.* 8(1):108. doi: [10.1038/s41392-023-01368-w](https://doi.org/10.1038/s41392-023-01368-w).
- Lim J, Luderer U. 2011. Oxidative damage increases and antioxidant gene expression decreases with aging in the mouse ovary. *Biol Reprod.* 84(4):775–782. doi: [10.1095/biolreprod.110.088583](https://doi.org/10.1095/biolreprod.110.088583).
- Liu H, Deng R, Zhu CW, Han HK, Zong GF, Ren L, Cheng P, Wei ZH, Zhao Y, Yu SY, et al. 2024. Rosmarinic acid in combination with ginsenoside Rg1 suppresses colon cancer metastasis via co-inhibition of COX-2 and PD1/PD-L1 signaling axis. *Acta Pharmacol Sin.* 45(1):193–208. doi: [10.1038/s41401-023-01158-8](https://doi.org/10.1038/s41401-023-01158-8).
- Liu XH, Cai SZ, Zhou Y, Wang YP, Han YJ, Wang CL, Zhou W. 2022. Ginsenoside Rg1 attenuates premature ovarian failure of D-gal induced POF mice through downregulating p16INK4a and upregulating SIRT1 expression. *Endocr Metab Immune Disord Drug Targets.* 22(3):318–327. doi: [10.2174/1871523020666210830164152](https://doi.org/10.2174/1871523020666210830164152).
- Luderer U, Lim J, Ortiz L, Nguyen JD, Shin JH, Allen BD, Liao LS, Malott K, Perraud V, Wingen LM, et al. 2022. Exposure to environmentally relevant concentrations of ambient fine particulate matter (PM2.5) depletes the ovarian follicle reserve and causes sex-dependent cardiovascular changes in apolipoprotein E null mice. *Part Fibre Toxicol.* 19(1):5. doi: [10.1186/s12989-021-00445-8](https://doi.org/10.1186/s12989-021-00445-8).
- Luo T, Jia X, Feng WD, Wang JY, Xie F, Kong LD, Wang XJ, Lian R, Liu X, Chu YJ, et al. 2023. Bergapten inhibits NLRP3 inflammasome activation and pyroptosis via promoting mitophagy. *Acta Pharmacol Sin.* 44(9):1867–1878. doi: [10.1038/s41401-023-01094-7](https://doi.org/10.1038/s41401-023-01094-7).
- Mansour KA, Elbermawi A, Al-Karmalawy AA, Lahloub MF, El-Neketi M. 2022. Cytotoxic effects of extracts obtained from plants of the Oleaceae family: bio-guided isolation and molecular docking of new secoiridoids from *Jasminum humile*. *Pharm Biol.* 60(1):1374–1383. doi: [10.1080/13880209.2022.2098346](https://doi.org/10.1080/13880209.2022.2098346).
- Mao Z, Liu S, Yu T, Su J, Chai K, Weng S. 2022. Yunpi Heluo decoction reduces ectopic deposition of lipids by regulating the SIRT1-FoxO1 autophagy pathway in diabetic rats. *Pharm Biol.* 60(1):579–588. doi: [10.1080/13880209.2022.2042567](https://doi.org/10.1080/13880209.2022.2042567).
- Mei J, Hao L, Liu X, Sun G, Xu R, Wang H, Liu C. 2019. Comprehensive analysis of peroxiredoxins expression profiles and prognostic values in breast cancer. *Biomark Res.* 7(1):16. doi: [10.1186/s40364-019-0168-9](https://doi.org/10.1186/s40364-019-0168-9).
- Mei M, Sun H, Xu J, Li Y, Chen G, Yu Q, Deng C, Zhu W, Song J. 2022. Vanillic acid attenuates H(2)O(2)-induced injury in H9c2 cells by regulating mitophagy via the PINK1/Parkin/Mfn2 signaling pathway. *Front Pharmacol.* 13:976156. doi: [10.3389/fphar.2022.976156](https://doi.org/10.3389/fphar.2022.976156).
- Meng Y, Qiu L, Zeng X, Hu X, Zhang Y, Wan X, Mao X, Wu J, Xu Y, Xiong Q, et al. 2022. Targeting CRL4 suppresses chemoresistant ovarian cancer growth by inducing mitophagy. *Signal Transduct Target Ther.* 7(1):388. doi: [10.1038/s41392-022-01253-y](https://doi.org/10.1038/s41392-022-01253-y).
- Mishra E, Thakur MK. 2023. Mitophagy: a promising therapeutic target for neuroprotection during ageing and age-related diseases. *Br J Pharmacol.* 180(12):1542–1561. doi: [10.1111/bph.16062](https://doi.org/10.1111/bph.16062).
- Nezis IP, Simonsen A, Sagona AP, Finley K, Gaumer S, Contamine D, Rusten TE, Stenmark H, Brech A. 2008. Ref(2)P, the *Drosophila melanogaster* homologue of mammalian p62, is required for the formation of protein aggregates in adult brain. *J Cell Biol.* 180(6):1065–1071. doi: [10.1083/jcb.200711108](https://doi.org/10.1083/jcb.200711108).
- Qin X, Chen H, Zhu X, Xu X, Gao J. 2023. Identification of Rab7 as an autophagy marker: potential therapeutic approaches and the effect of Qi



- Teng Xiao Zhuo granule in chronic glomerulonephritis. *Pharm Biol.* 61(1):1120–1134. doi: [10.1080/13880209.2023.2233998](https://doi.org/10.1080/13880209.2023.2233998).
- Shao YF, Tang BB, Ding YH, Fang CY, Hong L, Shao CX, Yang ZX, Qiu YP, Wang JC, Yang B, et al. 2023. Kaempferide ameliorates cisplatin-induced nephrotoxicity via inhibiting oxidative stress and inducing autophagy. *Acta Pharmacol Sin.* 44(7):1442–1454. doi: [10.1038/s41401-023-01051-4](https://doi.org/10.1038/s41401-023-01051-4).
- Shu F, Xiao H, Li QN, Ren XS, Liu ZG, Hu BW, Wang HS, Wang H, Jiang GM. 2023. Epigenetic and post-translational modifications in autophagy: biological functions and therapeutic targets. *Signal Transduct Target Ther.* 8(1):32. doi: [10.1038/s41392-022-01300-8](https://doi.org/10.1038/s41392-022-01300-8).
- Song C, Peng W, Yin S, Zhao J, Fu B, Zhang J, Mao T, Wu H, Zhang Y. 2016. Melatonin improves age-induced fertility decline and attenuates ovarian mitochondrial oxidative stress in mice. *Sci Rep.* 6(1):35165. doi: [10.1038/srep35165](https://doi.org/10.1038/srep35165).
- Sonn SK, Song EJ, Seo S, Kim YY, Um JH, Yeo FJ, Lee DS, Jeon S, Lee MN, Jin J, et al. 2022. Peroxiredoxin 3 deficiency induces cardiac hypertrophy and dysfunction by impaired mitochondrial quality control. *Redox Biol.* 51:102275. doi: [10.1016/j.redox.2022.102275](https://doi.org/10.1016/j.redox.2022.102275).
- Sun Z, Zhang H, Wang X, Wang QC, Zhang C, Wang JQ, Wang YH, An CQ, Yang KY, Wang Y, et al. 2018. TMCO1 is essential for ovarian follicle development by regulating ER Ca(2+) store of granulosa cells. *Cell Death Differ.* 25(9):1686–1701. doi: [10.1038/s41418-018-0067-x](https://doi.org/10.1038/s41418-018-0067-x).
- Takahashi M, Mizumura K, Gon Y, Shimizu T, Kozu Y, Shikano S, Iida Y, Hikichi M, Okamoto S, Tsuya K, et al. 2021. Iron-dependent mitochondrial dysfunction contributes to the pathogenesis of pulmonary fibrosis. *Front Pharmacol.* 12:643980. doi: [10.3389/fphar.2021.643980](https://doi.org/10.3389/fphar.2021.643980).
- Tang X, Zhong L, Tian X, Zou Y, Hu S, Liu J, Li P, Zhu M, Luo F, Wan H. 2023. RUNX1 promotes mitophagy and alleviates pulmonary inflammation during acute lung injury. *Signal Transduct Target Ther.* 8(1):288. doi: [10.1038/s41392-023-01520-6](https://doi.org/10.1038/s41392-023-01520-6).
- Tao X, Dou Y, Huang G, Sun M, Lu S, Chen D. 2021.  $\alpha$ -tubulin regulates the fate of germline stem cells in drosophila testis. *Sci Rep.* 11(1):10644. doi: [10.1038/s41598-021-90116-7](https://doi.org/10.1038/s41598-021-90116-7).
- Vazquez-Martin A, Van den Haute C, Cufi S, Corominas-Faja B, Cuyàs E, Lopez-Bonet E, Rodriguez-Gallego E, Fernández-Arroyo S, Joven J, Baekelandt V, et al. 2016. Mitophagy-driven mitochondrial rejuvenation regulates stem cell fate. *Aging.* 8(7):1330–1352. doi: [10.18632/aging.100976](https://doi.org/10.18632/aging.100976).
- Venkatachalam N, Bakavayev S, Engel D, Barak Z, Engel S. 2020. Primate differential redoxome (PDR) – a paradigm for understanding neurodegenerative diseases. *Redox Biol.* 36:101683. doi: [10.1016/j.redox.2020.101683](https://doi.org/10.1016/j.redox.2020.101683).
- Wang L, Tang XQ, Shi Y, Li HM, Meng ZY, Chen H, Li XH, Chen YC, Liu H, Hong Y, et al. 2023. Tetrahydroberberubine retards heart aging in mice by promoting PHB2-mediated mitophagy. *Acta Pharmacol Sin.* 44(2):332–344. doi: [10.1038/s41401-022-00956-w](https://doi.org/10.1038/s41401-022-00956-w).
- Wang S, Guo F, Ji Y, Yu M, Wang J, Li N. 2018. Dual-mode imaging guided multifunctional theranosomes with mitochondria targeting for photothermally controlled and enhanced photodynamic therapy in vitro and in vivo. *Mol Pharm.* 15(8):3318–3331. doi: [10.1021/acs.molpharmaceut.8b00351](https://doi.org/10.1021/acs.molpharmaceut.8b00351).
- Wang S, Long H, Hou L, Feng B, Ma Z, Wu Y, Zeng Y, Cai J, Zhang DW, Zhao G. 2023. The mitophagy pathway and its implications in human diseases. *Signal Transduct Target Ther.* 8(1):304.
- Weaver LN, Drummond-Barbosa D. 2021. Hormone receptor 4 is required in muscles and distinct ovarian cell types to regulate specific steps of *Drosophila* oogenesis. *Development.* 148(5):dev198663. doi: [10.1242/dev.198663](https://doi.org/10.1242/dev.198663).
- Xie Q, Zhang X, Zhou Q, Xu Y, Sun L, Wen Q, Wang W, Chen Q. 2023. Antioxidant and anti-inflammatory properties of ginsenoside Rg1 for hyperglycemia in type 2 diabetes mellitus: systematic reviews and meta-analyses of animal studies. *Front Pharmacol.* 14:1179705. doi: [10.3389/fphar.2023.1179705](https://doi.org/10.3389/fphar.2023.1179705).
- Xu X, Qu Z, Qian H, Li Z, Sun X, Zhao X, Li H. 2021. Ginsenoside Rg1 ameliorates reproductive function injury in C57BL/6J mice induced by di-N-butyl-phthalate. *Environ Toxicol.* 36(5):789–799. doi: [10.1002/tox.23081](https://doi.org/10.1002/tox.23081).
- Yang F, Zhang Y, Liu S, Xiao J, He Y, Shao Z, Zhang Y, Cai X, Xiong L. 2022. Tunneling nanotube-mediated mitochondrial transfer rescues nucleus pulposus cells from mitochondrial dysfunction and apoptosis. *Oxid Med Cell Longev.* 2022:3613319. doi: [10.1155/2022/3613319](https://doi.org/10.1155/2022/3613319).
- Yang N, Yu G, Lai Y, Zhao J, Chen Z, Chen L, Fu Y, Fang P, Gao W, Cai Y, et al. 2024. A snake cathelicidin enhances transcription factor EB-mediated autophagy and alleviates ROS-induced pyroptosis after ischaemia-reperfusion injury of island skin flaps. *Br J Pharmacol.* 181(7):1068–1090. doi: [10.1111/bph.16268](https://doi.org/10.1111/bph.16268).
- Yang SJ, Wang JJ, Cheng P, Chen LX, Hu JM, Zhu GQ. 2023. Ginsenoside Rg1 in neurological diseases: from bench to bedside. *Acta Pharmacol Sin.* 44(5):913–930. doi: [10.1038/s41401-022-01022-1](https://doi.org/10.1038/s41401-022-01022-1).
- Yu L, Wang Y, Guo YH, Wang L, Yang Z, Zhai ZH, Tang L. 2021. HIF-1 $\alpha$  alleviates high-glucose-induced renal tubular cell injury by promoting Parkin/PINK1-mediated mitophagy. *Front Med.* 8:803874. doi: [10.3389/fmed.2021.803874](https://doi.org/10.3389/fmed.2021.803874).
- Zhang H, Su Y, Sun Z, Chen M, Han Y, Li Y, Dong X, Ding S, Fang Z, Li W, et al. 2021. Ginsenoside Rg1 alleviates Abeta deposition by inhibiting NADPH oxidase 2 activation in APP/PS1 mice. *J Ginseng Res.* 45(6):665–675. doi: [10.1016/j.jgr.2021.03.003](https://doi.org/10.1016/j.jgr.2021.03.003).
- Zhang L, Yi H, Song J, Huang J, Yang K, Tan B, Wang D, Yang N, Wang Z, Li X. 2019. Mitochondria-targeted and ultrasound-activated nanodroplets for enhanced deep-penetration sonodynamic cancer therapy. *ACS Appl Mater Interfaces.* 11(9):9355–9366. doi: [10.1021/acsami.8b21968](https://doi.org/10.1021/acsami.8b21968).
- Zhang XW, Zhou JC, Jin CC. 2023. Mesaconine, a cardiotonic component of *Aconitum carmichaelii*, provides cardioprotection through enhancing PINK1-dependent cardiac mitophagy. *Brit J Pharmacol.* 180:68–69.
- Zhen J, Bai J, Liu J, Men H, Yu H. 2024. Ginsenoside RG1-induced mesenchymal stem cells alleviate diabetic cardiomyopathy through secreting exosomal circNOTCH1 to promote macrophage M2 polarization. *Phytother Res.* 38(4):1745–1760. doi: [10.1002/ptr.8018](https://doi.org/10.1002/ptr.8018).
- Zhou F, Song Y, Liu X, Zhang C, Li F, Hu R, Huang Y, Ma W, Song K, Zhang M. 2021. Si-Wu-Tang facilitates ovarian function through improving ovarian microenvironment and angiogenesis in a mouse model of premature ovarian failure. *J Ethnopharmacol.* 280:114431. doi: [10.1016/j.jep.2021.114431](https://doi.org/10.1016/j.jep.2021.114431).
- Zhou J, Xue Z, He HN, Liu X, Yin SY, Wu DY, Zhang X, Schatten H, Miao YL. 2019. Resveratrol delays postovulatory aging of mouse oocytes through activating mitophagy. *Aging.* 11(23):11504–11519. doi: [10.18632/aging.102551](https://doi.org/10.18632/aging.102551).
- Zhou JC, Jin CC, Wei XL, Xu RB, Wang RY, Zhang ZM, Tang B, Yu JM, Yu JJ, Shang S, et al. 2023. Mesaconine alleviates doxorubicin-triggered cardiotoxicity and heart failure by activating PINK1-dependent cardiac mitophagy. *Front Pharmacol.* 14:1118017. doi: [10.3389/fphar.2023.1118017](https://doi.org/10.3389/fphar.2023.1118017).
- Zhu T, Wang L, Wang LP, Wan Q. 2022. Therapeutic targets of neuroprotection and neurorestoration in ischemic stroke: applications for natural compounds from medicinal herbs. *Biomed Pharmacother.* 148:112719. doi: [10.1016/j.biopha.2022.112719](https://doi.org/10.1016/j.biopha.2022.112719).